

## Thermoelectric properties of perovskite-type rare earth cobalt oxide solid solutions $\text{Pr}_{1-x}\text{Dy}_x\text{CoO}_3$

Hideki Hashimoto<sup>a,b</sup>, Takafumi Kusunose<sup>c</sup> and Tohru Sekino<sup>b,\*</sup>

<sup>a</sup>The Institute of Scientific and Industrial Research, Osaka University, 8-1 Mihogaoka, Ibraki, Osaka 567-0047, Japan

<sup>b</sup>Institute of Multidisciplinary Research for Advanced Materials, Tohoku University, 2-1-1 Katahira, Aoba-ku, Sendai 980-8577, Japan

<sup>c</sup>Department of Advanced Materials Science, Faculty of Engineering, Kagawa University, 2217-20 Hayashi-cho, Takamatsu, 761-0396, Japan

Perovskite-type rare earth cobalt oxide  $\text{Pr}_{1-x}\text{Dy}_x\text{CoO}_3$  ( $x = 0, 0.25, 0.5, 0.75$  and  $1$ ) ceramics were fabricated by reaction sintering of the corresponding metal oxide powders, and their thermoelectric properties were evaluated up to 873 K. The electrical properties of  $\text{Pr}_{1-x}\text{Dy}_x\text{CoO}_3$  varied according to a variation in the  $x$  value, whereas the thermal conductivity of the solid solutions ( $x = 0.25 - 0.75$ ) tends to be lower than that of both end components ( $x = 0$  and  $1$ ). As the results,  $\text{Pr}_{0.75}\text{Dy}_{0.25}\text{CoO}_3$  ( $x = 0.25$ ) showed the highest figure of merit,  $Z = 5.72 \times 10^{-5} \text{ K}^{-1}$  at 773 K in the present  $\text{Pr}_{1-x}\text{Dy}_x\text{CoO}_3$  system. This is considered due mainly to the effect of decreasing thermal conductivity caused by phonon scattering of partially substituted A-site ions. These results suggest that the fabrication of solid solutions is effective in improving the thermoelectric properties of the  $\text{RCoO}_3$  system.

**Key words:** Thermoelectric properties, Perovskite, Rare earth cobalt oxides, Solid solutions, Phonon scattering.

### Introduction

The energy conversion performance of thermoelectric materials is usually characterized by the figure of merit  $Z$ , or the dimensionless figure of merit,  $ZT$  ( $T$ : absolute temperature)  $Z = S^2\sigma\kappa^{-1}$ , where  $S$  is the Seebeck coefficient,  $\sigma$  is the electrical conductivity, and  $\kappa$  is the thermal conductivity [1]. There are trade-off relations among these three parameters ( $S$ ,  $\sigma$ , and  $\kappa$ ), thus it is difficult to enhance the  $Z$  value. In general, a value of  $ZT$  greater than 1 is required for the practical application of thermoelectric materials [2, 3]. Only a few non-oxide materials, such as  $\text{Bi}_2\text{Te}_3$  and  $\text{Zn}_4\text{Sb}_3$ , fulfill that requirement [4]; they have been used in devices such as Peltier coolers. However, they contain toxic elements such as tellurium or antimony and non-oxide materials unstable at high temperatures or under oxidizing conditions. Therefore, oxide compounds that do not contain toxic elements are desirable for use at higher temperatures as thermoelectric materials and in devices used to convert geothermal or waste heat into electrical energy.

Previously, it was thought that oxide materials did not fulfill an appropriate electrical function for such applications because of their low carrier mobility, i.e., low electrical conductivity [5]. However, since the high thermoelectric performance of  $\text{Na}_x\text{CoO}_2$ , which was one of the strongly correlated electron systems with a layered structure, was

discovered [6], oxide thermoelectric materials have received much attention because they have rather good electrical properties but exhibit lower thermal conductivity than that of intermetallic compounds. It was reported that single crystal  $\text{Na}_x\text{CoO}_2$  exhibited a  $ZT$  value higher than 1 [7]. However, one can be aware that it has low chemical and thermal stability, resulting from hydration reactions under humid conditions and decomposition by volatilization of sodium at high temperatures. Thus, stable oxide thermoelectric materials need to be developed. Thus we have focused on the perovskite-type rare earth cobalt oxides ( $\text{RCoO}_3$ ) which are stable at high temperatures and under oxidizing conditions, and do not contain toxic elements. It has been reported that, among oxide ceramic materials,  $\text{RCoO}_3$ -based ceramics show a fairly good thermoelectric performance [8-11] regardless of their isotropic crystal structure.

As is easily deduced from the  $Z$  value equation mentioned above, reducing the thermal conductivity while increasing the electrical properties is usually desired to develop materials with better thermoelectric performances. Thermal conductivity  $\kappa$  consists of the carrier component  $\kappa_{\text{el}}$  and the phonon component  $\kappa_{\text{ph}}$ ;  $\kappa_{\text{el}}$  is a function of electrical conductivity as expressed by the Wiedemann-Franz law,  $\kappa_{\text{el}} = L\sigma T$  ( $L = 2.45 \times 10^8 \text{ WS}^{-1}\text{K}^{-2}$ : where  $L$  is the Lorenz number) [12]. On the other hand,  $\kappa_{\text{ph}}$  is not directly influenced by the carrier. Therefore, we thought that decreasing  $\kappa_{\text{ph}}$  by disordering the atomic arrangement or doping/substituting ions in the crystal would be effective for improving thermoelectric properties [13]. For this purpose, a solid solution technique and/or doping with

\*Corresponding author:  
Tel : +81-22-217-5832  
Fax: +81-22-217-5832  
E-mail: sekino@tagen.tohoku.ac.jp

different elements is often used, because the effect of certain types of phonon scattering caused by the doped/substituted ions would be expected due to the differences in atomic masses and atomic binding forces [14, 15]. Therefore, we expected that a controlled solid solution technique might be effective in decreasing thermal conductivity, that a design rule might be applicable also to perovskite cobalt oxides.

In this study, we aimed to decrease the thermal conductivity of  $\text{RCoO}_3$  ( $\text{R} = \text{Pr}$  and  $\text{Dy}$ ) by controlling the chemical composition of an A-site ion to form a solid solution between these phases.  $\text{Pr}_{1-x}\text{Dy}_x\text{CoO}_3$  compounds were fabricated by reaction sintering of the corresponding metal oxide powders. The effects of substitution of the  $\text{Pr}^{3+}$  ion by the smaller and heavier  $\text{Dy}^{3+}$  ion on the thermoelectric properties of these materials were investigated at temperatures up to 873 K.

## Experimental Procedure

$\text{Pr}_2\text{O}_3$ ,  $\text{Dy}_2\text{O}_3$ , and  $\text{Co}_3\text{O}_4$  (all 99.9% purity; Kojundo Chemical Laboratory, Saitama, Japan) were selected as raw materials and weighed in  $[(1-x)\text{Pr} + x\text{Dy}]/\text{Co} = 1$  ( $x = 0, 0.25, 0.5, 0.75, \text{ and } 1$ ) by the atomic ratio. They were mixed by wet and dry ball milling. These mixed powders were calcined in air at 973 K for 5 h. These calcined powders were compacted by uniaxial pressing (30 MPa) and cold isostatic pressing (200 MPa) to form disks 15 mm in diameter and 3 mm in thickness. The disks were then sintered in air at 1273 K for 8 h.

Crystalline phases and lattice constants of sintered samples were identified by X-ray diffraction (XRD) (RINT 2200; Rigaku, Kyoto, Japan) using the  $\text{Cu K}\alpha$  line. The density of the sintered samples was measured by the Archimedes' immersion method using toluene, and the relative density was then calculated using the measured and theoretical density values. The electrical conductivity ( $\sigma$ ) of the samples was measured by the van der Pauw method (ResiTest 8308; TOYO, Tokyo, Japan) from room temperature to 873 K under an air atmosphere. The Seebeck coefficient of the samples was measured by the conventional steady-state method using the same instrument as for the electrical conductivity measurements up to 873 K under an air atmosphere. Thermal diffusivity was measured using the laser flash method (TC-7000; ULVAC-RIKO, Tokyo, Japan), and the specific heat of the samples was measured by differential scanning calorimetry (DSC) (Model DSC404C; NETZSCH, Selb, Germany). Both measurements were performed under a high-purity Ar atmosphere up to 873 K. The thermal conductivity of the samples was then calculated from the product of thermal diffusivity, specific heat, and density values.

## Results and Discussion

To identify the crystalline phase of the samples prepared by reaction sintering, we carried out XRD analysis. Generally, the perovskite-type  $\text{RCoO}_3$  that contains the smaller R ions such as  $\text{Dy}^{3+}$  or  $\text{Ho}^{3+}$  is difficult to synthesize, and

the density of the sintered samples is rather low [9]. In the present  $\text{Pr}_{1-x}\text{Dy}_x\text{CoO}_3$  system, the perovskite-type single phase was not obtained for the sample of  $x = 1$  ( $\text{DyCoO}_3$ ) sintered at temperatures higher than 1323 K. Therefore all of the samples were sintered at 1273 K.

Fig. 1 shows the XRD patterns of the prepared samples sintered at 1273 K. The samples prepared at  $x = 0$  and 1 were identified as cubic perovskite-type  $\text{PrCoO}_3$  and orthorhombic perovskite-type  $\text{DyCoO}_3$ , respectively; these results were in good agreement with values in the JCPDS-International Centre for Diffraction Data [16]. At  $x = 0.25$ – $0.75$ , the crystalline structure has a tendency to change from cubic to orthorhombic with increasing  $x$  values, and no impurity phase was detected. By analyzing the XRD patterns in detail, the samples of  $x = 0.25$  and  $0.5/0.75$  were assigned as cubic and orthorhombic structures, respectively. These results indicate that the solid solutions of two type rare earths containing cobalt oxides  $\text{Pr}_{1-x}\text{Dy}_x\text{CoO}_3$  were successfully fabricated.

The lattice constant and lattice volume of  $\text{Pr}_{1-x}\text{Dy}_x\text{CoO}_3$  calculated from the XRD patterns are shown in Fig. 2. The lattice constant changed systematically with increasing  $x$  values; the lattice constants of  $a$ - and  $c$ -axes decreased

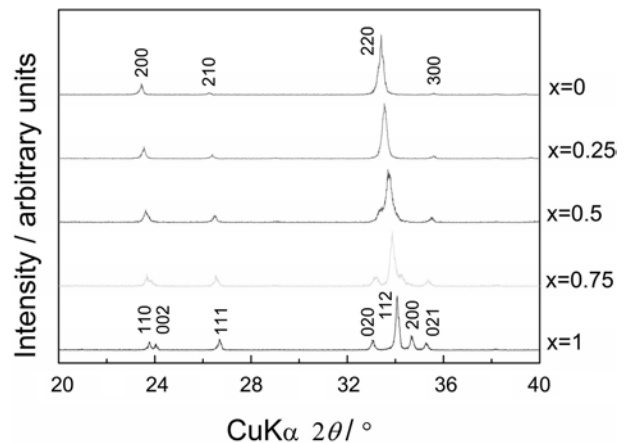


Fig. 1. XRD patterns of the prepared samples sintered at 1273 K.

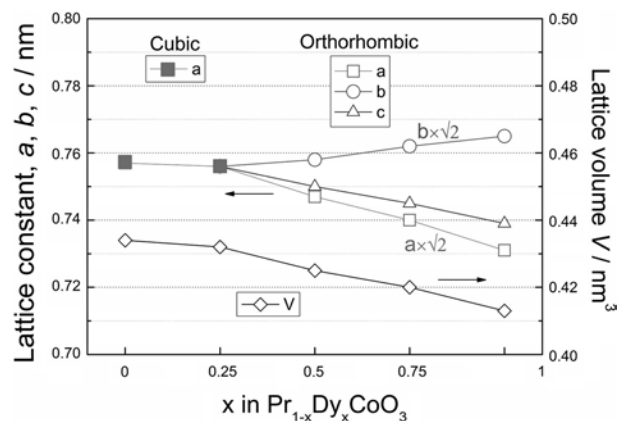


Fig. 2. Lattice constants and lattice volume of  $\text{Pr}_{1-x}\text{Dy}_x\text{CoO}_3$  ( $x = 0, 0.25, 0.5, 0.75$  and  $1$ ), where, the constants for the orthorhombic phase are depicted as  $a \times \sqrt{2}$  and  $b \times \sqrt{2}$  to compare with those of cubic phase, and the volume ( $V$ ) was calculated using the depicted constants.

while that of b-axis increased, and as a result, the lattice volume decreased with increasing  $x$  values. The ionic radii of  $\text{Pr}^{3+}$  and  $\text{Dy}^{3+}$  are 132 pm and 124 pm (in twelve-coordination) respectively [17], therefore, the decrease of lattice volume with increasing of  $x$  values is regarded as the decrease of the average ionic size of the R-site by substituting the  $\text{Dy}^{3+}$  for the  $\text{Pr}^{3+}$  ion, and accordingly the unit cell becomes distorted from cubic to orthorhombic symmetry. As to the sintered density of  $\text{Pr}_{1-x}\text{Dy}_x\text{CoO}_3$ , all of the samples were sintered at 1273 K to obtain single phase as mentioned above, consequently their relative density was rather low. Besides, the relative density of solid solutions ( $x = 0.25 - 0.75$ ) tend to show a lower value than that of  $x = 0$  and 1; the values were 54.9, 52.5, and 51.1% for  $x = 0.25, 0.5$ , and 0.75 while 67.6 and 64.4% for  $x = 0$  and 1, respectively.

We measured the electrical conductivity of  $\text{Pr}_{1-x}\text{Dy}_x\text{CoO}_3$ , which is one of the constituents of the thermoelectric figure of merit. Fig. 3 shows the electrical conductivity of the prepared samples. The temperature dependence of the electrical conductivity shows semiconductive behavior; it increased with increasing temperature. By comparing the electrical conductivity at the same test temperature, it is found that the  $\sigma$  value decreased with increasing  $x$  values. As discussed above, the perovskite-type unit cell structure of  $\text{Pr}_{1-x}\text{Dy}_x\text{CoO}_3$  became distorted from cubic to orthorhombic with the decreasing average ionic radii of the rare earth elements at the A-site. It has been reported that the angles of the Co-O-Co bonds decreased from  $180^\circ$  as the ionic radii of the rare earth elements decreased, for example the angles are around  $158^\circ$  for  $\text{PrCoO}_3$  and  $149^\circ$  for  $\text{DyCoO}_3$  [18], respectively. The decrease of the angles caused a reduction in the overlap between the cobalt  $3d$  and the oxygen  $2p$  orbital in the corner-shared  $\text{CoO}_6$  octahedra [19-23]. Therefore, it is considered that the distortion of the perovskite-type structure of  $\text{Pr}_{1-x}\text{Dy}_x\text{CoO}_3$  causes the decrease in the electrical conductivity.

We also measured the Seebeck coefficient of  $\text{Pr}_{1-x}$

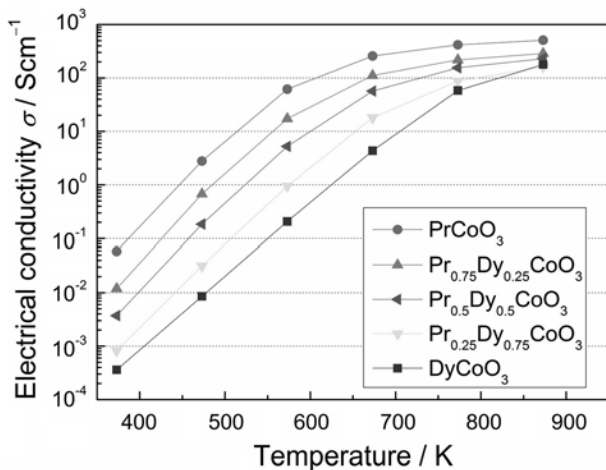


Fig. 3. Electrical conductivity of  $\text{Pr}_{1-x}\text{Dy}_x\text{CoO}_3$  ( $x = 0, 0.25, 0.5, 0.75$  and  $1.0$ ) as a function of test temperature.

$\text{Dy}_x\text{CoO}_3$ . Fig. 4 shows the Seebeck coefficient of the prepared samples. Since the value of  $S$  for the present system is positive over the entire range measured, the major conduction carrier is a hole, thus representing a p-type semiconductor. The Seebeck coefficient of these samples decreased with increasing temperature, and at the same temperature it increased with increasing  $x$  values. In general, in semiconductors, the Seebeck coefficient tends to decrease when the electrical conductivity increases owing to increasing carrier concentration; this is also true for the present case with the trade-off relationship between  $\sigma$  and  $S$ .

We then measured the thermal conductivity ( $\kappa$ ) of  $\text{Pr}_{1-x}\text{Dy}_x\text{CoO}_3$  and calculated the carrier components of the thermal conductivity ( $\kappa_{\text{el}}$ ) of  $\text{Pr}_{1-x}\text{Dy}_x\text{CoO}_3$  ( $\kappa = \kappa_{\text{el}} + \kappa_{\text{ph}}$ ; where  $\kappa_{\text{ph}}$  is the phonon component of thermal conductivity [12]). Figs. 5 and 6 show the measured  $\kappa$  and the calculated  $\kappa_{\text{el}}$  of  $\text{Pr}_{1-x}\text{Dy}_x\text{CoO}_3$ , respectively. The carrier component of the thermal conductivity ( $\kappa_{\text{el}}$ ) of the samples

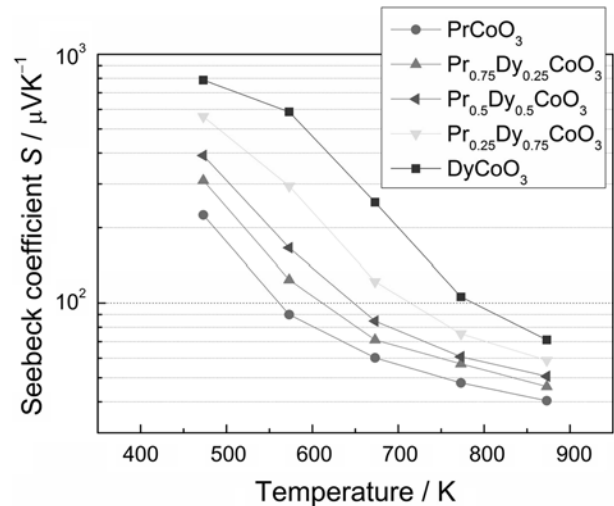


Fig. 4. Seebeck coefficient of  $\text{Pr}_{1-x}\text{Dy}_x\text{CoO}_3$  ( $x = 0, 0.25, 0.5, 0.75$  and  $1.0$ ) as a function of test temperature.

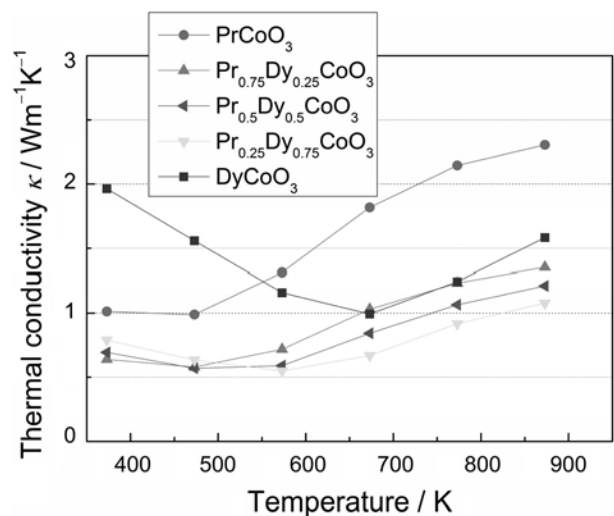
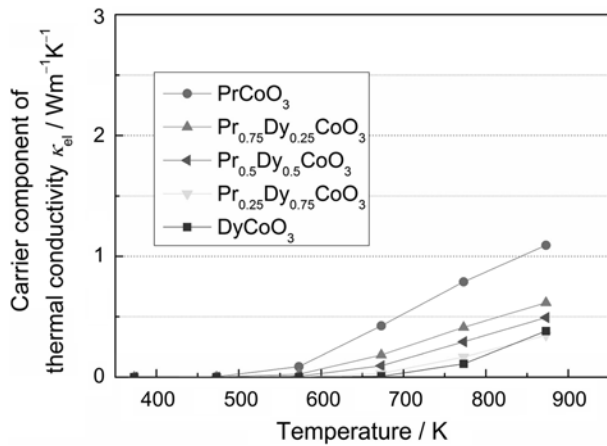


Fig. 5. Thermal conductivity of  $\text{Pr}_{1-x}\text{Dy}_x\text{CoO}_3$  ( $x = 0, 0.25, 0.5, 0.75$  and  $1.0$ ) as a function of test temperature.



**Fig. 6.** Carrier component of thermal conductivity ( $\kappa_{el}$ ) of  $\text{Pr}_{1-x}\text{Dy}_x\text{CoO}_3$  ( $x = 0, 0.25, 0.5, 0.75$  and  $1.0$ ) calculated from the electrical conductivity data as a function of test temperature.

was calculated using the electrical conductivity ( $\sigma$ ) values via the Wiedemann-Franz law expressed as follows [12]:

$$\kappa_{el} = L\sigma T \quad (1)$$

where  $L$  is the Lorentz number ( $= 2.45 \times 10^{-8} \text{ WS}^{-1}\text{K}^{-2}$ ) and  $T$  is the measured temperature. By comparing the thermal conductivity variation of the end members ( $x = 0$  and  $1$ ) from Fig. 5, the  $\kappa$  value of  $\text{PrCoO}_3$  ( $x = 0$ ) is lower than that of  $\text{DyCoO}_3$  ( $x = 1$ ) up to  $473 \text{ K}$  while the relation is changed above  $573 \text{ K}$ , i.e.  $\text{DyCoO}_3$  ( $x = 1$ ) shows lower  $\kappa$  value. For the solid solutions, ( $x = 0.25 - 0.75$ ), the  $\kappa$  curves tend to show a lower value than that of  $x = 0$  and  $1$  for the entire temperature range in this study. On the other hand, it is evident from Fig. 6 that the carrier contribution ( $\kappa_{el}$ ) becomes more dominant at higher temperatures, which is a typical characteristic of semiconductors. Moreover,  $\kappa_{el}$  tends to decrease with increasing  $x$  values; i.e., with the progress of  $\text{Dy}^{3+}$  substitution for  $\text{Pr}^{3+}$ . As discussed above, the perovskite-type unit cell structure of  $\text{Pr}_{1-x}\text{Dy}_x\text{CoO}_3$  became distorted from cubic to orthorhombic with increasing  $x$  values, and it causes a decrease in the electrical conductivity. This effect directly contributes to the decrease in  $\kappa_{el}$ , which can be calculated using equation (1).

The above-mentioned facts indicate that the lower values obtained for  $\kappa$  for the solid solutions were caused by the decreased contribution of  $\kappa_{ph}$  and not by that of  $\kappa_{el}$ . Values of  $\kappa_{ph}$  tend to be influenced by phonon scattering due to the substituted A-site ions, while those of  $\kappa_{el}$  tend to be influenced by the distortion of the perovskite structure. It is well known that the atomic mass as well as ionic size differences and defect formation are responsible for the phonon scattering (thermal resistivity) of solid solutions. In the present system, Pr has a larger ionic radius ( $132 \text{ pm}$  [17]) and a lower atomic mass ( $140.9$  [24]) than those of Dy ( $124 \text{ pm}$  [17] and  $162.5$  [24], respectively). Therefore, it is considered that both the size and mass play important roles in phonon scattering on the reduced thermal con-

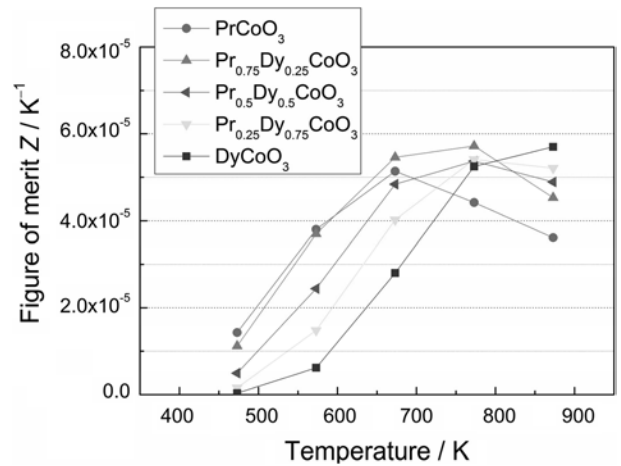


**Fig. 7.** Figure of merit of  $\text{Pr}_{1-x}\text{Dy}_x\text{CoO}_3$  ( $x = 0, 0.25, 0.5, 0.75$  and  $1.0$ ) as a function of test temperature.

ductivity of the solid solution. In addition, it is rationalized that the decrease of relative density of solid solutions also contributes to the decrease in  $\kappa_{ph}$ .

Conversely, defect formation and its contribution to the decreased thermal conductivity in the present solid solution may be small, because both Pr and Dy are considered as trivalent cations that do not, in principle, form oxygen defects. To evaluate the thermoelectric performance of  $\text{Pr}_{1-x}\text{Dy}_x\text{CoO}_3$ , we calculated the figure of merit ( $Z$ ) from the data of the electrical conductivity, the Seebeck coefficient, and the thermal conductivity. Fig. 7 shows the calculated  $Z$ . At  $773 \text{ K}$ , the  $Z$  of the solid solutions ( $x = 0.25 - 0.75$ ) tend to show higher values than that of the end members ( $x = 0$  and  $1$ ), and  $\text{Pr}_{0.75}\text{Dy}_{0.25}\text{CoO}_3$  ( $x = 0.25$ ) showed the highest figure of merit,  $Z = 5.72 \times 10^{-5} \text{ K}^{-1}$  at  $773 \text{ K}$  in the present  $\text{Pr}_{1-x}\text{Dy}_x\text{CoO}_3$  system. As discussed above, the phonon component of the thermal conductivity of solid solutions decreased by both the phonon scattering of partially substituted A-site ions and the lower relative density. On the other hand, the lower thermal conductivity due to the lower density hardly contributes to enhance the thermoelectric performance because it brings a significant decrease in electrical properties [25]. Therefore the results are considered due mainly to the effect of decreasing thermal conductivity caused by phonon scattering.

## Conclusion

The substitution of Pr ions at the A-site by Dy in  $\text{Pr}_{1-x}\text{Dy}_x\text{CoO}_3$  resulted in a gradual change in the crystalline structure of perovskite-type  $\text{RCO}_3$  from cubic to orthorhombic, which are the typical crystal structures of each end member,  $\text{PrCoO}_3$  and  $\text{DyCoO}_3$ , respectively. The electrical conductivity and the Seebeck coefficient of  $\text{Pr}_{1-x}\text{Dy}_x\text{CoO}_3$  decreased and increased with increasing  $x$  values, respectively, whereas the thermal conductivity of  $\text{Pr}_{1-x}\text{Dy}_x\text{CoO}_3$ , with  $x = 0.25 - 0.75$ , was lower than that of the end members, with  $x = 0$  and  $1$ , at almost all test temperatures. As the results, the solid solution  $\text{Pr}_{0.75}\text{Dy}_{0.25}\text{CoO}_3$  ( $x = 0.25$ )

showed the highest thermoelectric performance (figure of merit),  $Z = 5.72 \times 10^{-5} \text{ K}^{-1}$  at 773 K in the present  $Pr_{1-x}Dy_xCoO_3$  system. This is considered due mainly to the effect of decreasing the thermal conductivity caused by phonon scattering of partially substituted A-site ions. These results suggest that the fabrication of solid solutions is effective in improving the thermoelectric properties of the  $RCO_3$  system.

### References

1. G. Chen, M.S. Dresselhaus, G. Dresselhaus, J.-P. Fleurial and T. Caillat, *Int. Mater. Rev.* 48[1] (2003) 45-66.
2. S. Ohta, T. Nomura, H. Ohta and K. Koumoto, *J. Appl. Phys.* 97[3] (2005) 034106.
3. K. Kurosaki, T. Sekimoto, K. Kawano, H. Muta and S. Yamanaka, *J. Jpn. Powder Powder Metall.* 54[5] (2007) 370-374.
4. T. Caillat, J.-P. Fleurial and A. Borshchevsky, *J. Phys. Chem. Solids* 58[7] (1997) 1119-1125.
5. N. Murayama and K. Koumoto, *Bull. Ceram. Soc. Jpn.* 33[3] (1998) 161-165.
6. I. Terasaki, Y. Sasago and K. Uchinokura, *Phys. Rev. B* 56[20] (1997) R12685-R12687.
7. K. Fujita, T. Mochida and K. Nakamura, *Jpn. J. Appl. Phys.* 40[7] (2001) 4644-4647.
8. J.-W. Moon, W.-S. Seo, H. Okabe, T. Okawa and K. Koumoto, *J. Mater. Chem.* 10[9] (2000) 2007-2009.
9. J.-W. Moon, Y. Masuda, W.-S. Seo and K. Koumoto, *Mater. Lett.* 48[3-4] (2001) 225-229.
10. J.-W. Moon, Y. Masuda, W.-S. Seo and K. Koumoto, *Mater. Sci. Eng. B* 85[1] (2001) 70-75.
11. H. Hashimoto, T. Kusunose and T. Sekino, *J. Alloy. Compd.* 484[1-2] (2009) 246-248.
12. J.R. Drabble and H.J. Goldsmid, in "Thermal Conduction in Semiconductors" (Pergamon Press, 1961) pp. 7-12.
13. S. Katsuyama and H. Okada, *J. Jpn. Soc. Powder Powder Metall.* 54[5] (2007) 375-380.
14. W.D. Kingery, H.K. Bowen and D.R. Uhlmann, in "Introduction to Ceramics" 2nd edition (Wiley-Interscience, 1976) pp.615-624.
15. N.P. Padture and P.G. Klemens, *J. Am. Ceram. Soc.* 80[4] (1997) 1018-1020.
16. JCPDS-International Centre for Diffraction Data, PDF No. 25-1069 and 25-1051.
17. Y.Q. Jia, *J. Solid State Chem.* 95[1] (1991) 184-187.
18. J.A. Alonso, M.J. Martínez-Lope, C. de la Calle and V. Pomjakushin, *J. Mater. Chem.*, 16[16] (2006) 1555-1560.
19. J. Zannen, G.A. Sawatzky and J.W. Allen, *Phys. Rev. Lett.* 55[4] (1985) 418-421.
20. J. Zannen and G.A. Sawatzky, *J. Solid State Chem.* 88[1] (1990) 8-27.
21. J.B. Torrance, P. Lacorre, A.I. Nazzari, E.J. Ansaldo, Ch. Niedermayer, *Phys. Rev. B* 45[14] (1992) 8209-8212.
22. T. Arima, Y. Tokura, J.B. Torrance, *Phys. Rev. B* 48[23] (1993) 17006-17009.
23. G. Ch. Kostoglou and N. Vasilakos, *Ch. Ftikos, Solid State Ionics* 106[3-4] (1998) 207-218.
24. International Union of Pure and Applied Chemistry, in "Quantities, Units, and Symbols in Physical Chemistry" 3rd edition (RSC Publishing, 2007) pp. 117-120.
25. H. Ohta, *Bull. Ceram. Soc. Jpn.* 42[8] (2007) 592-595.